



Dual-etch apodised grating couplers for efficient fibre-chip coupling near 1310 nm wavelength

XIA CHEN,* DAVID J. THOMSON, LEE CRUDGINTON, ALI Z. KHOKHAR, AND GRAHAM T. REED

Optoelectronics Research Centre, University of Southampton, University Road, Southampton, Hampshire SO17 1BJ, UK

*xia.chen@soton.ac.uk

Abstract: We present our recent work on fibre-chip grating couplers operating around 1310 nm. For the first time, we demonstrate the combination of dual-etch and apodization design approaches which may achieve a coupling efficiency of 85% (−0.7 dB). Subwavelength structures were employed to modify the coupling strength of the grating. −1.9 dB efficiency was measured from a first set of fabricated structures.

Published by The Optical Society under the terms of the [Creative Commons Attribution 4.0 License](https://creativecommons.org/licenses/by/4.0/). Further distribution of this work must maintain attribution to the author(s) and the published article's title, journal citation, and DOI.

OCIS codes: (230.3120) Integrated optics devices; (250.5300) Photonic integrated circuits; (050.2770) Gratings.

References and links

1. D. Taillaert, F. Van Laere, M. Ayre, W. Bogaerts, D. Van Thourhout, P. Bienstman, and R. Baets, "Grating couplers for coupling between optical fibers and nanophotonic waveguides," *Jpn. J. Appl. Phys.* **45**(8A), 6071–6077 (2006).
2. W. S. Zaoui, A. Kunze, W. Vogel, M. Berroth, J. Butschke, F. Letzkus, and J. Burghartz, "Bridging the gap between optical fibers and silicon photonic integrated circuits," *Opt. Express* **22**(2), 1277–1286 (2014).
3. C. Sun, M. Georgas, J. Orcutt, B. Moss, Y.-H. Chen, J. Shainline, M. Wade, K. Mehta, K. Nammari, E. Timurdogan, D. Miller, O. Tehar-Zahav, Z. Sternberg, J. Leu, J. Chong, R. Bafrali, G. Sandhu, M. Watts, R. Meade, M. Popović, R. Ram, and V. Stojanović, "A monolithically-integrated chip-to-chip optical link in bulk CMOS," *IEEE J. Solid-State Circuits* **50**(4), 828–844 (2015).
4. R.-J. Essiambre, R. Ryf, N. K. Fontaine, and S. Randel, "Breakthroughs in photonics 2012: space-division multiplexing in multimode and multicore fibers for high-capacity optical communication," *IEEE Photonics J.* **5**(2), 0701307 (2013).
5. D.-X. Xu, J. H. Schmid, G. T. Reed, G. Z. Mashanovich, D. J. Thomson, M. Nedeljkovic, X. Chen, D. Van Thourhout, S. Keyvaninia, and S. K. Selvaraja, "Silicon photonic integration platform – Have we found the sweet spot?" *IEEE J. Sel. Top. Quantum Electron.* **20**(4), 189–205 (2014).
6. X. Chen, C. Li, C. K. Y. Fung, S. M. G. Lo, and H. K. Tsang, "Apodized waveguide grating couplers for efficient coupling to optical fibers," *IEEE Photonics Technol. Lett.* **22**(15), 1156–1158 (2010).
7. D. Vermeulen, S. Selvaraja, P. Verheyen, G. Lepage, W. Bogaerts, P. Absil, D. Van Thourhout, and G. Roelkens, "High-efficiency fiber-to-chip grating couplers realized using an advanced CMOS-compatible silicon-on-insulator platform," *Opt. Express* **18**(17), 18278–18283 (2010).
8. D. Benedikovic, C. Alonso-Ramos, P. Cheben, J. H. Schmid, S. Wang, D.-X. Xu, J. Lapointe, S. Janz, R. Halir, A. Ortega-Moñux, J. G. Wangüemert-Pérez, I. Molina-Fernández, J.-M. Fédéli, L. Vivien, and M. Dado, "High-directionality fiber-chip grating coupler with interleaved trenches and subwavelength index-matching structure," *Opt. Lett.* **40**(18), 4190–4193 (2015).
9. N. Na, H. Frish, I.-W. Hsieh, O. Harel, R. George, A. Barkai, and H. Rong, "Efficient broadband silicon-on-insulator grating coupler with low backreflection," *Opt. Lett.* **36**(11), 2101–2103 (2011).
10. R. Shi, H. Guan, A. Novack, M. Streshinsky, A. E.-J. Lim, G.-Q. Lo, T. Baehe-Jones, and M. Hochberg, "High-Efficiency Grating Couplers Near 1310nm Fabricated by 248-nm DUV Lithography," *IEEE Photonics Technol. Lett.* **26**(15), 1569–1572 (2014).
11. R. Halir, P. Cheben, J. H. Schmid, R. Ma, D. Bedard, S. Janz, D.-X. Xu, A. Densmore, J. Lapointe, and I. Molina-Fernández, "Continuously apodized fiber-to-chip surface grating coupler with refractive index engineered subwavelength structure," *Opt. Lett.* **35**(19), 3243–3245 (2010).
12. X. Chen and H. K. Tsang, "Polarization-independent grating couplers for silicon-on-insulator nanophotonic waveguides," *Opt. Lett.* **36**(6), 796–798 (2011).
13. R. Halir, P. Cheben, S. Janz, D.-X. Xu, I. Molina-Fernández, and J. G. Wangüemert-Pérez, "Waveguide grating coupler with subwavelength microstructures," *Opt. Lett.* **34**(9), 1408–1410 (2009).

14. X. Chen and H. Tsang, "Nanoholes grating couplers for coupling between silicon-on-insulator waveguides and optical fibers," IEEE Photonics J. **1**(3), 184–190 (2009).
15. R. Orobtcchouk, A. Layadi, H. Gualous, D. Pascal, A. Koster, and S. Laval, "High-efficiency light coupling in a submicrometric silicon-on-insulator waveguide," Appl. Opt. **39**(31), 5773–5777 (2000).

1. Introduction

The grating coupler is a key component used for coupling between optical fibres and photonic waveguides in photonic circuits [1, 2]. Improving the coupling efficiency of grating couplers is critical to meet the overall power budget for an optical communication link [3]. Compared to butt-coupling techniques, grating couplers can work without any back-end processing, such as facet polishing and coating. Further advantages are that they enable wafer-scale testing, allow better flexibility in circuit layout and have a greater tolerance to alignment errors. In addition to the simplicity in device design and fabrication, grating couplers can also be utilized for many unique applications, such as coupling to multi-mode and multi-core fibres [4].

For a basic grating coupler, the fundamental optical mode from the photonic waveguide is first expanded laterally by an adiabatic taper to a waveguide with a width of approximately 10 μm , which matches the mode size of single-mode optical fibre. The light is then coupled by grating diffraction into the optical fibre. The grating period needed for out-of-plane coupling to the fibre is calculated by the phase matching condition.

Much work has been done to improve the coupling efficiency of grating couplers around 1550nm wavelengths (C-band). The top silicon thickness and etch depth can be optimised to achieve high directionality [5, 6] (defined as the portion of optical power coupled upwards to the fibre) for single-etch gratings. Alternatively, a substrate mirror [2], an additional layer of poly-silicon [7], or interleaved trenches [8] can also greatly improve the coupling efficiency.

Unfortunately, according to our two dimensional finite-difference time-domain (2D FDTD) simulations, with the commonly available silicon-on-insulator (SOI) platform with 220 nm top-silicon thickness, single-etch grating couplers can only achieve a directionality of 0.71 with 2 μm buried oxide layer for the 1310nm wavelength band (O-band). This wavelength band is widely used in short-range board-to-board or rack-to-rack links for data centres. A few results were demonstrated recently [9, 10]. The grating coupler design presented by Na *et al.* [9] is based on a 400 nm top-silicon wave-guiding thickness, which is not widely adopted and only -3 dB efficiency was achieved. Shi *et al.* [10] improved the coupling efficiency by employing two etch depths and varying each period to achieve an output mode which matches the fibre mode. However, as there is only one etch depth for each grating period, the efficiency is still limited by the directionality.

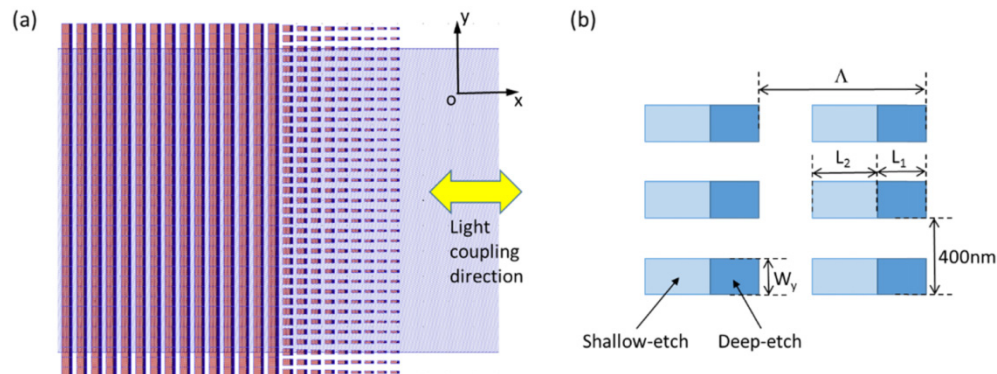


Fig. 1. (a) An illustration of the fabricated dual-etch apodised fibre-chip grating couplers. (b) A detailed illustration of the subwavelength structures in the front part of the grating coupler.

In this work, we make use of the 70 nm shallow-etch process, which is generally used for standard single-etch grating couplers [1, 2], and the 120 nm shallow-etch process generally for defining the rib waveguide, to design dual-etch gratings to improve the directionality of coupling. The lateral fill factor f_y was tuned based on the theory for subwavelength structures [11, 12] to apodise the coupling strength and optimise the coupling efficiency. Grating couplers formed by subwavelength structures were first proposed [13] and experimentally demonstrated [14] in 2009. It provides us another degree of freedom while designing the grating coupler. As shown in Fig. 1, the coupling strength along the x-axis was then apodised to achieve a Gaussian-like output optical mode to match the mode profile of a standard optical fibre. The design layout of the grating coupler is shown in Fig. 1.

2. Grating designs and optimizations

2D FDTD simulations were used to simulate the grating diffraction [6, 12]. Grating couplers presented in this paper were optimised for coupling with only the transverse-electric (TE) mode with a centre wavelength of 1310 nm. The devices are designed based on Silicon-on-Insulator (SOI) wafers with a 220 nm thick top silicon layer and a 2 μm thick buried oxide layer (BOX). Fibres were aligned to the surface of the SOI wafer with a tilting angle of $\theta = 10^\circ$ off normal when assuming index matching gel applied on top of grating couplers. In order to simplify the fabrication process and reduce cost, only a 70 nm etching step and a 120 nm etching step are employed for our design. The 70 nm etching process is provided in most silicon photonics foundries, which is optimized for the standard single-etch grating couplers [1, 2]. The 120 nm etching process was primarily used to form the rib waveguides, which could have P/N implantations in the slab region to form active devices, such as MZI modulators. A 1000 nm thick PECVD silicon dioxide cladding was deposited on top of the photonic devices.

A similar approach as [8] using interleaved trenches based on 70 nm and 120 nm etch (Fig. 2(a)) was first explored to improve the directionality of the grating coupler. Simulations show that with the 70 nm deep and 120 nm deep trenches, grating couplers can only reach a maximum of 0.85 directionality with the optimum design. The directionality can be improved to 0.95, when the 120 nm and 70 nm deep etch windows are overlapped to achieve 190 nm deep trenches for the grating couplers, which is illustrated in Fig. 2(b). There is a 1000 nm oxide cladding on top the grating coupler, which is omitted in the Fig. 2. We only fabricated and experimentally characterized the grating coupler design in Fig. 2(b), as it has a better performance according to our simulations.

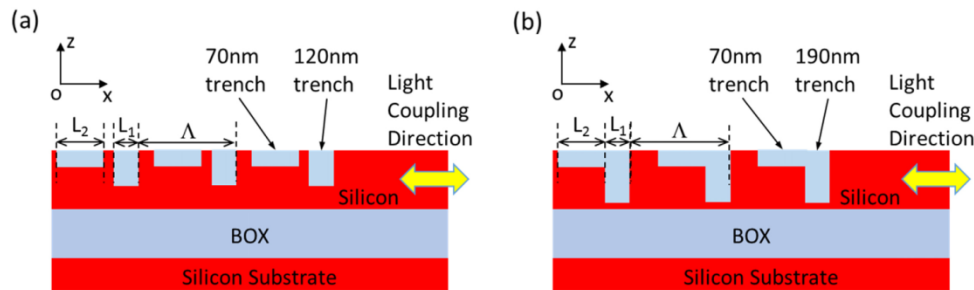


Fig. 2. (a) Cross-section (side-view) of dual-etch grating couplers with interleaved trenches of 70nm and 120nm depth. (b) Cross-section (side-view) of dual-etch grating couplers with trenches of 70nm and 190nm depth, which can achieve better directionality. This design is fabricated and experimentally characterized.

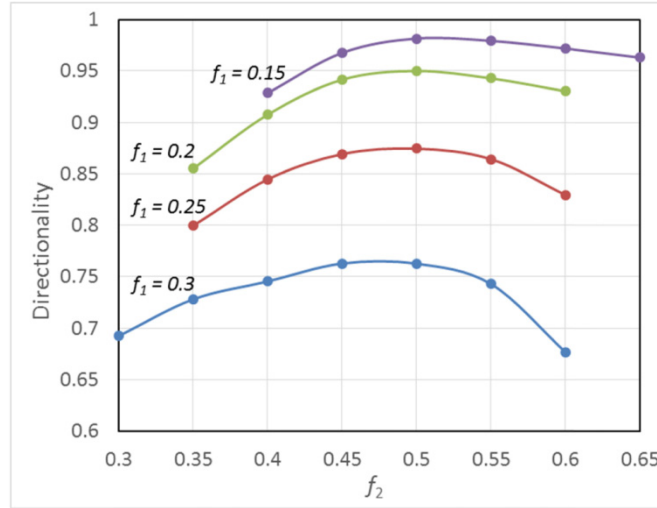


Fig. 3. The calculated directionality of the grating coupler for various fill factors for the deep-etched trenches f_1 and fill factors for the shallow-etched trenches f_2 .

A series of parameters for the grating coupler were adjusted to achieve the optimised directionality. As shown in Fig. 2(b), we define the fill factor $f_1 = L_1 / \Lambda$, which is the ratio in width of the deep-etched trench over the grating period, and fill factor $f_2 = L_2 / \Lambda$, which is the ratio in width of the shallow-etched trench over the grating period. According to our simulations as shown in Fig. 3, the directionality achievable increases with reducing fill factor of the deep-etched trench f_1 until an optimum value at 0.98 with $f_1 = 0.15$ is reached. Then the directionality achievable will decrease with decreasing f_1 when $f_1 < 0.15$.

The period of the grating coupler can be as small as 500 nm in our design. In order to make the devices less demanding on the fabrication process and enable them to be possibly fabricated with widely available Deep-VU photo lithography processes, we would like to keep the minimum dimension of the trenches above 100 nm, which will sacrifice the directionality by 0.02. This corresponds to a minimum fill factor of 0.2 for the both f_1 and f_2 . Therefore, we set $f_1 = 0.2$ and $f_2 = 0.5$ for our design, which gives a directionality of 0.95.

In addition to the directionality, which counts the percentage of light coupling upwards to the fibre, the mode matching efficiency between the profile of out-coupled light and the fundamental mode in the optical fibre is also a key parameter that limits the coupling efficiency. For uniform grating couplers, the out-coupled light profile would have an exponential decay pattern due to constant coupling strength along the grating. This would induce significant coupling loss due to the mode mismatch with the Gaussian-like fibre mode [1]. Techniques to apodise the coupling strength of the grating coupler and achieve a Gaussian-like out-coupled light profile can dramatically improve the coupling efficiency [6, 11].

The optical power confined in the grating structure may be described by $P(x) = P_0 e^{-2\alpha x}$ along the x-axis due to the continuous leaking (coupling) of light, where $P(x)$ is the optical power guided in the grating waveguide at position x , P_0 is the launched power at the starting point of the grating coupler, and α is defined as the coupling strength. The mode matching efficiency (overlap integral) could only reach a maximum of 80% with a Gaussian-shaped fibre mode with optimized design, when α is equal to approximately $0.15 \mu\text{m}^{-1}$ for fibre with $9.2 \mu\text{m}$ mode field diameter (MFD) [15]. Higher coupling efficiency could be achieved by varying the coupling strength of the grating coupler along the x-axis to obtain a Gaussian-shaped output field profile $G(x)$. Thus we can have: $dP(x)/dx = -2\alpha P(x) = -G^2(x)$. α is then calculated shown in Eq. (1).

$$\alpha(x) = \frac{G^2(x)}{2\left(1 - \int_0^x G^2(t)dt\right)} \quad (1)$$

Since the etch depths and fill factors (f_1 , f_2) have already been optimized to enhance directionality as described above, we introduce subwavelength structures to modify the coupling strength along the x-axis as shown in Fig. 1. Both the shallow and deep trenches were changed into subwavelength structures laterally (in y-direction) for the first few periods of the grating coupler, which can reduce the coupling strength of the grating depending on the lateral fill factor. The period in y-direction is set to 400 nm, which is smaller than the wavelength in the grating structure. We define a lateral fill factor $f_y = W_y / (400 \text{ nm})$ as shown in Fig. 1(b), which is the ratio of the etched groove width over the subwavelength period in y direction. A 2nd-order approximation of the effective medium theory (EMT) [12] was employed to calculate the effective index of the subwavelength structures. The calculated indices were then used for 2D FDTD simulations for the grating coupler. In the apodised grating coupler design, the lateral fill factor f_y was modified to change the coupling strength according to Eq. (1).

The calculated results for different lateral fill factors, f_y were shown in Fig. 4. Because of the reasons described previously regarding the fabrication, we would like to keep the minimum trench width above 100 nm, and therefore the minimum f_y is 0.25. This leads to a minimum coupling strength of $0.025 \mu\text{m}^{-1}$. The corresponding grating period is 511 nm according to the phase matching condition of grating diffraction. When f_y is gradually increased to 1, the coupling strength α is also gradually increased to $0.167 \mu\text{m}^{-1}$. The corresponding grating period for coupling at 1310 nm is increased to 584 nm. The simulation results for those parameters is shown in Fig. 4.

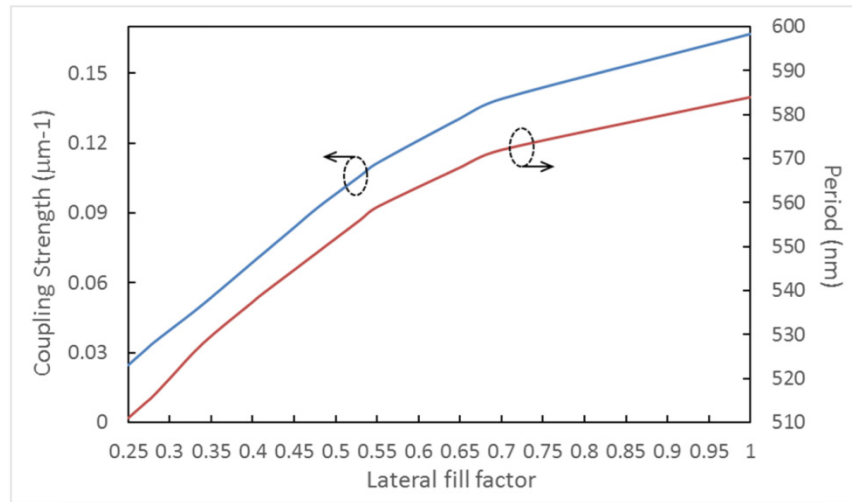


Fig. 4. Coupling strength and grating period versus lateral fill factor f_y for coupling at 1310nm wavelength with $f_1 = 0.2$ and $f_2 = 0.5$.

Table 1. Detailed design parameters for the optimised dual-etch subwavelength grating coupler. The coupling strength α was apodised along x-axis by adjusting f_y with $f_1 = 0.2$ and $f_2 = 0.5$.

| Grating No. | 1 | 2 | 3 | 4 | 5 | 6 | 7 | 8 | 9 | ≥ 10 |
|-----------------------------|-------|-------|-------|------|-------|-------|-------|-------|-------|-----------|
| $\alpha (\mu\text{m}^{-1})$ | 0.025 | 0.025 | 0.031 | 0.04 | 0.053 | 0.068 | 0.085 | 0.106 | 0.131 | 0.167 |
| Period (nm) | 511 | 511 | 514 | 520 | 530 | 537 | 545 | 556 | 568 | 584 |
| f_y | 0.25 | 0.25 | 0.27 | 0.3 | 0.35 | 0.4 | 0.45 | 0.53 | 0.65 | 1 |

The detailed design of the optimized dual-etch apodised grating couplers is listed in Table 1. We define the first period of the grating at the light input/output end as grating number 1, and count each period accordingly. The coupling strength was apodised according to Eq. (1) along the x-axis for each grating period by adjusting the lateral fill factor f_y . The period of the grating was then calculated by the phase matching condition and verified with FDTD simulations. With the grating design shown in Table 1, a maximum predicted coupling efficiency of 85% (-0.7 dB) was achieved. The result is shown in Fig. 5. According our simulations, the overlap integral between the grating coupler output and the fundamental fibre mode is improved to 90%. The back reflection is reduced to 0.7% while coupling from waveguide into the grating coupler.

The simulation result of an optimized uniform dual-etch subwavelength grating coupler was also plotted in the Fig. 5 as a comparison. The lateral fill factor f_y was set to 0.65 for all the grating periods of the uniform design, which offers with a constant coupling strength α of $0.131 \mu\text{m}^{-1}$. The period of the gratings was 568nm .

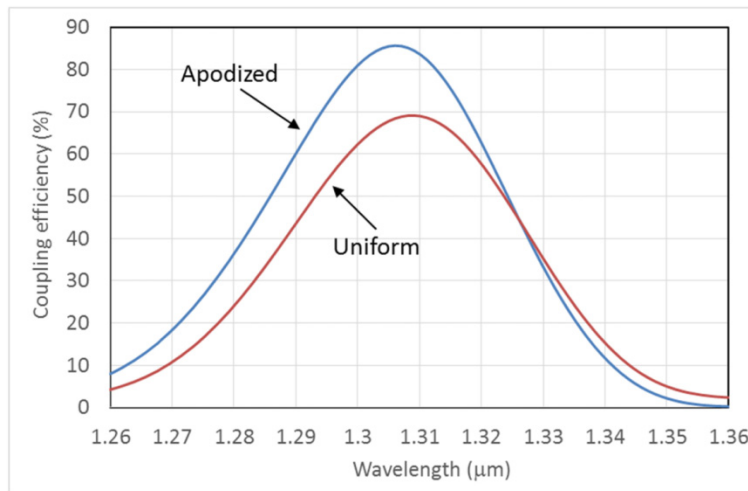


Fig. 5. Calculated coupling efficiency of the apodized dual-etch subwavelength grating coupler and a uniform dual-etch subwavelength grating coupler with $f_y = 0.65$.

3. Experimental measurement

The fabrication was performed in the nanofabrication cleanrooms at the University of Southampton, and E-beam lithography was used for defining the gratings. However, as we kept all dimensions larger than 100 nm, the grating designs are compatible with DUV lithography processes as used for high volume production. The two Si etching processes were carried out by inductively coupled plasma (ICP) dry etcher. We first defined and etched the 70 nm depth patterns and then did the 120 nm depth etch. The 190 nm depth patterns were created by overlapping the patterns of both etch steps. A SEM image of a typical dual-etch apodised grating coupler fabricated is shown in Fig. 6.

We characterized the fabricated grating couplers by measuring the fibre-waveguide-fibre insertion loss of the optical signal. A 400 μm long linear taper with negligible loss is used for converting the optical mode from the 12 μm waveguide with gratings to a 500 nm wide single-mode waveguide. The input/output grating couplers including the linear tapers were connected with a 200 μm long and 500 nm wide single-mode waveguide. The coupling efficiency of each grating coupler was obtained simply by taking half of the fibre-to-fibre loss, assuming that the coupling efficiencies were the same for the couplers at both ends and neglecting the waveguide propagation loss of the 200 μm long waveguide.

We achieved -1.9 dB peak coupling efficiency with the optimized design as listed in Table 1, with a 1 dB bandwidth of 23 nm. As shown in Fig. 7, no strong FP effect was observed around the centre wavelength, indicating the back reflection of the grating to the waveguide is significantly reduced. Index matching gel (G608N3 from Thorlabs) with an index of 1.44, which is the same as the oxide cladding, was applied to reduce the reflections from the chip surface and the fibre facet during experimental measurement.

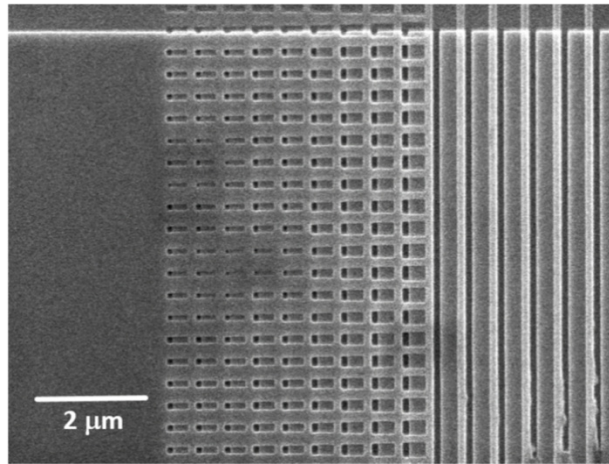


Fig. 6. SEM image of a typical dual-etch apodised grating coupler.

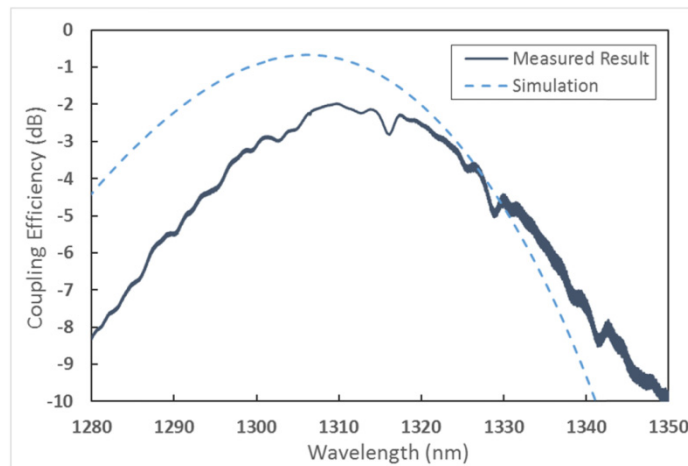


Fig. 7. Measured coupling efficiency for the dual-etch apodised grating coupler. The simulation result (in dB scale) was plotted for reference.

There is some difference between the measured and simulated results. This is most likely due to the variations in the fabrication processes, such as the angle of the etched side-walls, variations in dimensions, and overlay shift between those two etch steps because of inaccurate mask alignment. According to our simulation, over 0.3 dB loss can be induced solely by the 20 nm overlay tolerance from our E-beam facility. Another 0.4 dB loss can be induced by 10 nm error in etch depths. We were using cleaved fibres that were tilted at 10 degree for our measurement, the distance between the centre of the fibre facet and the grating coupler is at least 11 μm . This will also induce about 0.3 dB loss because of the mode expansion in free space. Further improvement in coupling efficiency is possible by fine tuning the process parameters and improving the experimental set-up.

Instead of our proposed design, alternative approaches such as adding a substrate mirror [2] or a poly-silicon overlay [7] can also possibly improve the directionality for 1310 nm wavelength, but at the cost of several additional fabrication processes.

4. Summary

We presented our recent work on fibre-chip grating couplers operating around 1310 nm. A dual-etch process, which utilises the etch processes originally designed for fabrication of waveguides and grating couplers, was adopted to enhance the directionality of coupling. We also apodised the gratings by using subwavelength structures to further enhance the coupling efficiency, through increased mode matching with the optical fibre and reduced back reflection to the waveguide. A coupling efficiency of 85% (-0.7 dB) was suggested with FDTD simulations, although our characterisation of the first fabricated structures has demonstrated a result of -1.9 dB coupling efficiency.

Funding

The Engineering and Physical Sciences Research Council (EPSRC) (EP/L00044X/1).

Acknowledgments

Reed is a Royal Society Wolfson Research Merit Award holder and thanks the Wolfson Foundation and the Royal Society for funding the award. DJT acknowledges funding from the Royal Society for his University Research Fellowship.